ELSEVIER

PALAEO

Palaeogeography, Palaeoclimatology, Palaeoecology 157 (2000) 109–125

www.elsevier.nl/locate/palaeo

'Cold' stage formation of calcrete nodules in the Chinese Loess Plateau: evidence from U-series dating and stable isotope analysis

P.J. Rowe, B.A. Maher *

School of Environmental Sciences, University of East Anglia, Norwich NR4 7TJ, UK

Received 7 February 1999; accepted for publication 4 October 1999

Abstract

This pilot study shows that some calcrete nodules from the base of palaeosols in the Chinese loess sequences can be dated by U-series isochron methods. The ages obtained suggest that the nodules did not form during interglacial climate stages; rather, they formed either during interglacial/glacial transitions or glacial climate stages. Thus, the nodules appear not to have formed contemporaneously with the soils beneath which they immediately lie but significantly post-date them. Post-pedogenic injection of carbonate into stratigraphically lower horizons is therefore identified. This finding contradicts previous assumptions regarding the timing of nodule formation. Carbon and oxygen isotope analyses of the nodules identify isotopic compositions which independently suggest that climatic conditions cooler and possibly drier than at present prevailed at the time of nodule formation.

Keywords: calcrete nodules; Chinese loess; palaeosol; stable isotopes; uranium series dating

1. Introduction

The interbedded loess/palaeosol sequences of the Loess Plateau of north-central China (Fig. 1) constitute the most complete terrestrial geological record of the Quaternary Period so far known. Palaeoclimatic data retrieved from these sediments, via a variety of geological proxy indicators (including magnetic properties, stable isotopes, granulometry and malacology), identify significant fluctuations of climate and environment during the Quaternary. During 'interglacial' periods, the rain-bearing east Asian summer monsoon was generally relatively strong, the region (particularly the presently sub-arid western Plateau) was wetter and soil-forming processes dominated. During 'glacial' periods, the south-east monsoon generally weakened, the dry north-west winter monsoon was more dominant, soil-forming processes weakened or ceased and loess accumulated on the Plateau. However, high-resolution magnetic, grain size and carbonate data from the western Loess Plateau (Chen et al., 1997) and palynological data (Sun et al., 1997) also identify significant climatic and environmental changes *within* individual climate stages. For example, Chen et al. (1997) identify some time periods (e.g. 70–50 ka) when both the summer and winter monsoons were relatively weak. During such times, cooler but moist climate conditions probably existed in the

* Corresponding author. Tel.: +44-1603-5931-22; fax: +44-1603-507719.

E-mail addresses: p.rowe@uea.ac.uk (P.J. Rowe), b.maher@uea.ac.uk (B.A. Maher)

0031-0182/00/$ - see front matter
PII: S0031-0182(99)00157-1

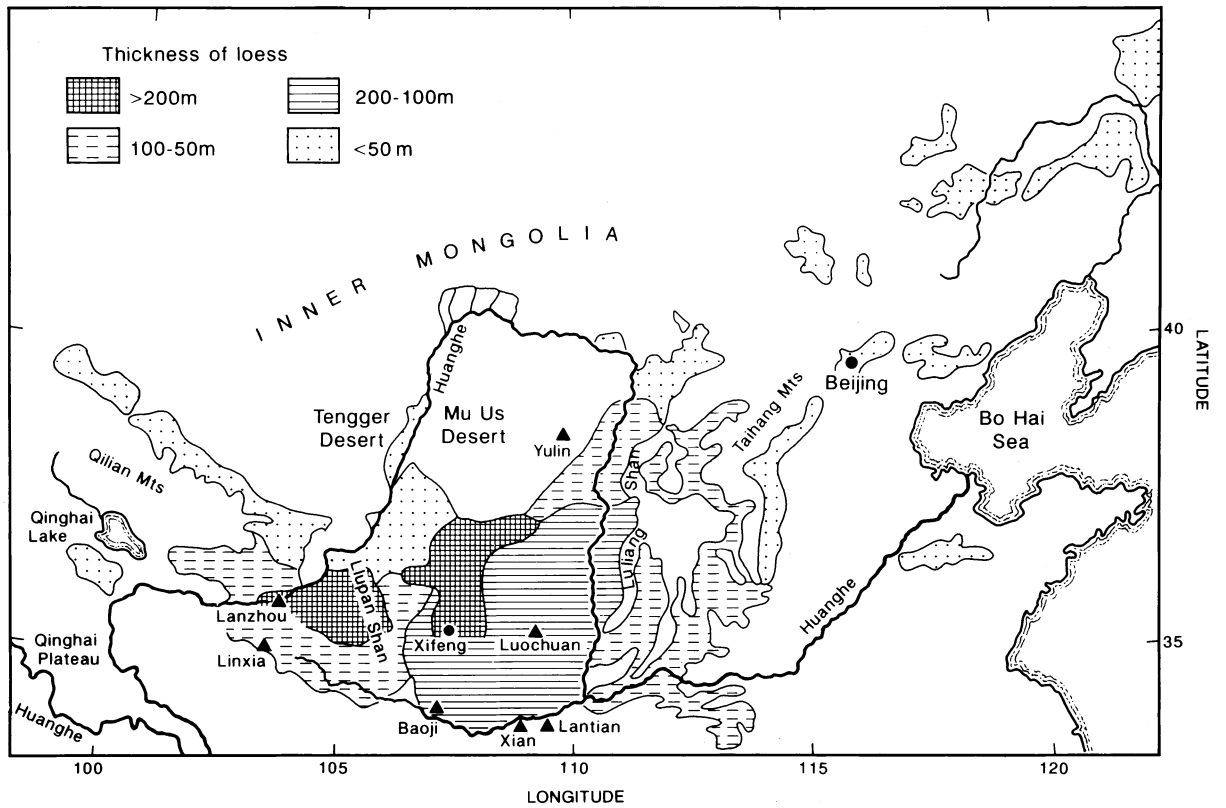

Fig. 1. Map of the Chinese Loess Plateau.

western Loess Plateau. Similarly, Sun et al.'s (1997) palynological data indicate a succession of steppe and meadow-steppe environments in the Loess Plateau over the last 100 ka, with short intervals of forest development even during 'cold' climate stages (e.g. *Ulmus* at ~95–91 ka, *Corylus* at ~25–21 ka, *Tsuga* at ~14–12 ka).

To obtain quantitative data on palaeoclimatic and palaeoecological changes in the region, several authors (e.g. Wang and Zheng, 1989; Frakes and Sun, 1994; Han et al., 1997; Wang et al., 1997) have used stable isotope analysis of the secondary carbonate cements and nodules which commonly occur within the loess/palaeosol sequences. The $\delta^{18}O$ and $\delta^{13}C$ signatures of the carbonate have been used to estimate average annual temperature, the isotopic composition of precipitation and the relative proportions of C_3 and C_4 plants growing on the Plateau at any given time. Such reconstructions clearly require a reliable chronological framework before they can be fully exploited.

We report here the results of a pilot study to investigate the potential for dating, by the uranium–thorium method, of calcrete nodules, commonly found at the base of the palaeosols in the Chinese Loess Plateau. Studies elsewhere have shown that dating of such detritally-contaminated carbonates can play an important role in establishing the chronology of stratigraphic sequences (Bischoff et al., 1988; Szabo et al., 1989; Kaufman, 1971; Kaufman et al., 1992). Here, we attempt to apply U-series methods to calcrete nodules from the upper part (0 to ~350 ka) of the Chinese loess sequences. In addition, carbon and oxygen isotopic analyses of the calcrete nodules have been carried out. These analyses enable us to compare their isotopic signatures with those previously reported for nodules from across the Chinese Loess Plateau,

and thence obtain independent and complementary palaeoenvironmental data on the dated nodules.

2. The nature and significance of pedogenic carbonates

The origins of pedogenic calcrete nodules are imperfectly understood. It is generally believed that calcium carbonate is leached from the soil profile by porewaters with relatively high dissolved CO_2 content (from plant decay and root respiration), and transported in solution down the soil profile. Following this dissolution and eluviation, reprecipitation of carbonate occurs at some depth, usually >25 cm (Cerling and Quade, 1993), in the B or C horizon. Precipitation of carbonate occurs when the soil solution becomes supersaturated with respect to calcite. Supersaturation can result from several possible factors, including: increases in the concentrations and activities of dissolved calcium and hydrogen carbonate due to water loss by evaporation or evapotranspiration; decreased $p(CO_2)$ leading to degassing of CO_2 from the soil solution; and microbial activity (Cerling and Quade, 1993). Estimates vary as to the amount of annual precipitation required for pedogenic carbonate formation; they generally lie in the range 400–750 mm (Cerling, 1984). However, rather than the amounts of rainfall per se, a seasonally wet/dry climate, with a critical balance between rainfall and evaporation, is considered to be a key factor in driving calcrete formation (Rossinsky and Swart, 1993).

In the loess/palaeosol sequences of the Chinese Loess Plateau (where individual loess and soil units are conventionally labelled by counting down from the top, S_0, S_1 etc), calcrete nodules occur towards the base of many of the palaeosols [e.g. Fig. 2(a)]. Notably, however, nodules are absent from palaeosol S_{5-1} (one of the most reddened soils in the sequence); conversely, nodules also occur within some of the relatively unweathered loess layers. In the Loess Plateau region, most rainfall occurs during the monsoonal summer months. In the relatively wetter central and south-eastern areas (present annual rainfall $\sim$500–800 mm), the nodules are well-developed, with dimensions in excess

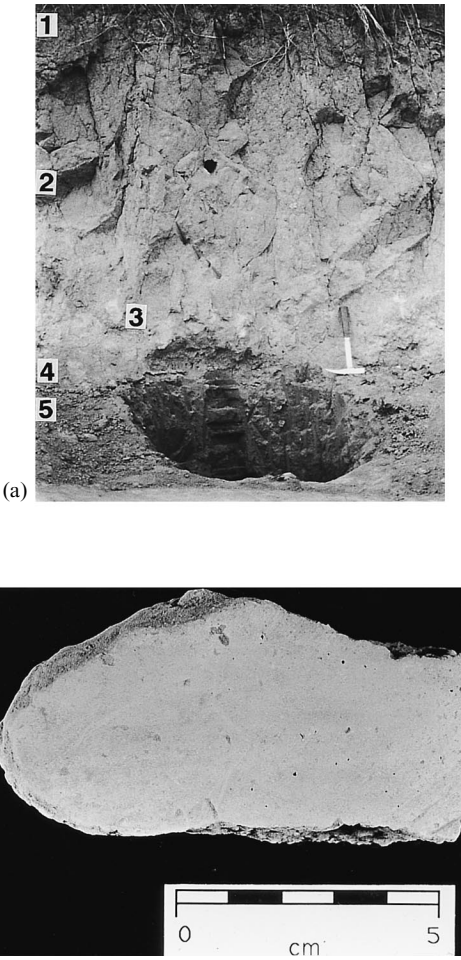

Fig. 2. (a) Photograph of the upper $\sim$3.5 m of the sequence at Liujiapo, showing: 1, upper palaeosol; 2, weakly weathered loess; 3, upper calcrete nodule layer; 4, narrow loess layer; and 5; well-developed palaeosol. (b) Photograph of a sampled nodule from Luochuan.

of 10 cm [Fig. 2(b)]. In the drier western area (annual rainfall $\sim$200–400 mm), nodule formation appears to have been restricted; where they occur, they are only a few millimetres in size. This spectrum of climate-dependent development, and their common stratigraphic location (at the base of soil profiles), suggests they have a pedogenic rather than groundwater origin (Gu et al., 1991; Wang and Zheng, 1989; Zheng et al., 1987). Critically, it has so far been assumed that nodule formation in the Loess Plateau proceeded contemporaneously with soil development.

3. Stratigraphy and sampling

The geography of the Loess Plateau is shown in Fig. 1. Nodules were sampled from beneath palaeosols S_1, S_{2-1} and S_{2-2} from Luochuan (35.7°N 109.8°E), near the centre of the plateau. Samples were also obtained from below two palaeosols within the upper part of the sequence at Liujiapo, near Xi'an, on the south-eastern fringe of the Plateau, a site for which thermoluminescence ages have been reported (Musson et al., 1994). Liujiapo (34.2°N 109.2°E) is sited on a NE-facing terrace of the Ba river, a tributary of the Hwang-Ho (Yellow River). The terrace consists of >100 m of loess and interbedded palaeosols, overlying alluvial gravels.

In their luminescence study of the upper 5.5 m of the Liujiapo section, Musson et al. (1994) identified a red-brown palaeosol at ~5.3 m, which they dated at 55.1 ka (i.e. within oxygen isotope stage 3). Their age model interprets this palaeosol as an interstadial soil developed within loess layer L_1. Musson et al. concluded that the overlying 'loess' was deposited at a fairly constant rate between 51 and 15 ka. However, other workers (e.g. Sun and Li, 1986) have identified an additional, younger palaeosol in this section, at ~2.75 to 0.5 m depth. The presence of this younger palaeosol is supported both by our magnetic susceptibility record for this site [Fig. 3(a)] and the age–depth curve constructed from Musson et al.'s luminescence data [Fig. 3(b)]. Higher values of magnetic susceptibility [associated with pedogenic formation of magnetite, for example, Maher (1998)] occur at this depth interval; it is also associated with a significantly lower rate of sediment accumulation. Calcrete nodules are also found at the base of this upper palaeosol. For this study, calcrete nodules were sampled from ~2.75 m depth, below the upper palaeosol, and

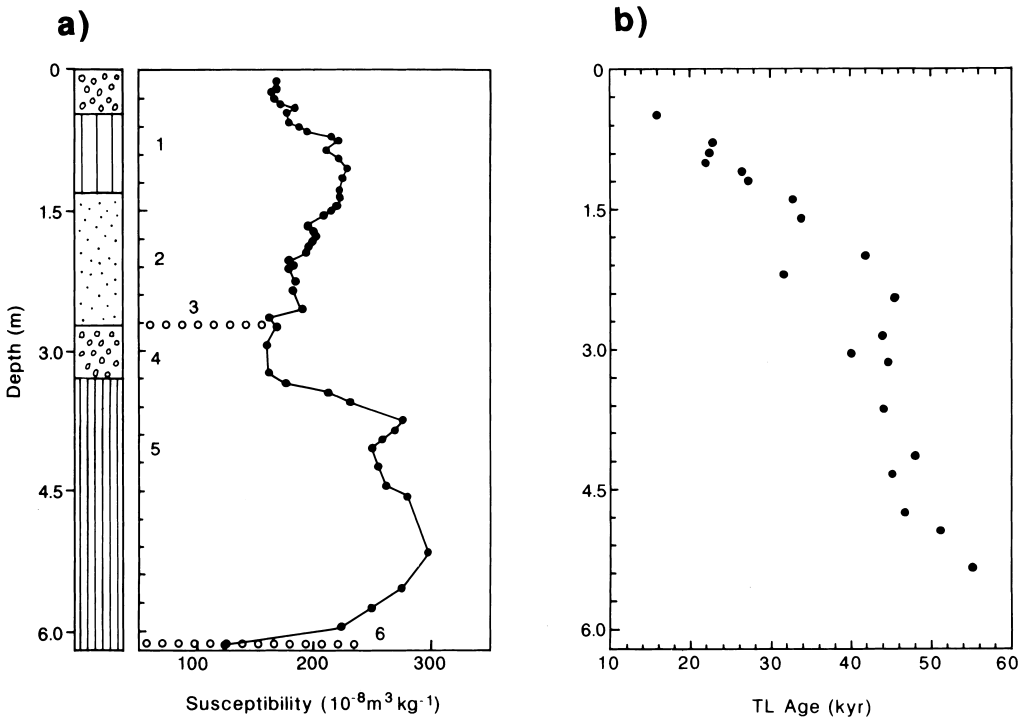

Fig. 3. (a) Lithological and magnetic susceptibility records for the upper 6 m of the Liujiapo section. [Key to lithology as in Fig. 2(a): 1, upper palaeosol; 2, weakly weathered loess; 3, upper calcrete nodule layer; 4, narrow loess layer; 5, well-developed palaeosol; and 6, lower calcrete nodule layer (sampled for U-series analysis)]. (b) Age–depth curve constructed from published TL dates (Musson et al., 1994).

from ~6.0 m depth, below the lower palaeosol [Fig. 3(a)].

The sampled nodules [e.g. Fig. 2(b)] from both Luochuan and Liujiapo were 5–10 cm across, very hard and displayed no obvious growth layers in hand specimen. Carbonate content was ~40%. Microscopic examination of thin sections using cathodoluminescence microscopy revealed a brown, non-luminescent micritic ground mass, throughout which were dispersed detrital grains of feldspar and carbonate. These detrital grains, coarse silt to fine sand in size, comprised ~5% of the calcrete volume. The feldspar grains were mostly unetched whilst the carbonate grains showed evidence of corrosion and micritic re-entrants around the margins, indicating that the calcitic ground mass is replacive. Much of the calcrete consists of quartz grains with micritic coatings. The microstructure of the calcretes can be classified as alpha fabrics (Wright and Tucker, 1991) since biogenic features were not observed.

4. Principles and methodology

4.1. Uranium–thorium dating of pedogenic carbonates

Uranium-thorium dating relies on the propensity of uranium, a very soluble element in oxidised groundwaters, to co-precipitate with calcium during carbonate formation, in the absence of its daughter, ^{230}Th, which is almost totally immobile in the near-surface environment (Langmuir and Herman, 1980). The subsequent ingrowth of ^{230}Th provides a chronometer with which to measure elapsed time since carbonate deposition. Age is calculated from the measured ^{230}Th/^{234}U and ^{234}U/^{238}U ratios in the sample (Ivanovich and Harmon, 1992).

The ingrowth of ^{230}Th to secular equilibrium with its parent ^{234}U takes ca. 350 ka and sets the upper age limit for the technique. Preconditions for the reliability of the calculated age are that no thorium should initially be present and that the carbonate must remain a closed system after deposition, allowing no isotopic migration across its boundaries. The presence of any initial thorium can be deduced from the presence of the cosmogenic isotope ^{232}Th and thus this potential source of error can be detected.

Many types of carbonate precipitates, such as speleothems and many corals, can be dated reliably by this method (Latham and Schwarcz, 1992). Pedogenic carbonates are more difficult to date; they often contain a high proportion of detrital particles which, upon sample dissolution, contribute sufficient amounts of uranium and thorium isotopes to obscure the authigenic carbonate signal. The theory of dating such detritally contaminated carbonates has been discussed in detail by Ku and Liang (1984), Schwarcz and Latham (1989), Bischoff and Fitzpatrick (1991) and Luo and Ku (1991) and applications to pedogenic carbonates reported (e.g. Ku et al., 1979; Szabo et al., 1989). Kaufman (1991) has discussed some of the proposed correction methods. Ages for such carbonates can be derived from isochrons constructed using isotopic data from several subsamples. Plotting the data in ^{230}Th/^{232}Th versus ^{234}U/^{232}Th and ^{234}U/^{232}Th versus ^{238}U/^{232}Th space will define mixing lines joining the carbonate and detrital end members, providing:

1. they are composed of simple mixtures of isotopically homogenous end members (i.e. detritus containing ^{234}U, ^{238}U, ^{230}Th and ^{232}Th, and carbonate containing all these isotopes except ^{232}Th);
2. the carbonate fraction contained only uranium isotopes at the time of deposition; and
3. the degree of isotopic fractionation between soluble and insoluble phases is constant for all leached subsamples.

The gradient of regression lines fitted to the data will provide the ^{230}Th/^{234}U and ^{234}U/^{238}U ratios, respectively, of the pure carbonate component of the sample (Schwarcz and Latham, 1989). However, the two isotope ratio plots (i.e. ^{230}Th/^{232}Th versus ^{234}U/^{232}Th and ^{234}U/^{232}Th versus ^{238}U/^{232}Th) share a common axis and thus the fitted regression lines are not statistically independent. The three-dimensional maximum-likelihood regression procedure of Ludwig and Titterington (1994) is statistically more rigorous. This routine has been incorporated into the ISOPLOT program of Ludwig (1994), which has been used here to

derive the reported ages. Errors are derived from a Maximum Likelihood Estimation of the uncertainty of fit of the isochron, based on the standard deviations of the measured isotope ratios.

4.2. Stable isotopes in pedogenic carbonates

The carbon isotope composition of soil carbonates is controlled by the composition of CO_2 in the soil atmosphere, which in turn is dictated mainly by the relative proportions of C_3 and C_4 plants in the local ecosystem (Cerling and Quade, 1993). C_3 plants (trees, most shrubs and herbs and cool season grasses) produce organic matter with $\delta^{13}C$ values of ca. -25 to $-32‰$ whilst the equivalent C_4 value (for plants such as prairie and savannah grasses) is ca. -10 to $-14‰$ (Deines, 1980). Following isotopic enrichment, due to diffusion processes, and isotopic fractionation between the soil CO_2 and precipitating carbonate, soil carbonates will possess $\delta^{13}C$ values of ca. $-12‰_{PDB}$ in pure C_3 ecosystems and $+2‰$ in pure C_4 ecosystems (Cerling and Quade, 1993).

The $\delta^{18}O$ values of soil carbonates from a wide range of climate zones have been shown to be highly correlated with the composition of the local meteoric water (Cerling, 1984; Cerling and Quade, 1993). In turn, the isotopic composition of meteoric water is strongly correlated with temperature (Rozanski et al., 1993), although other factors, such as continentality and the amount of precipitation, can significantly modify this relationship.

5. Laboratory methods

5.1. U-series

The sampled nodules were sectioned by sawing and pulverised in a disc mill. In this pilot study, one nodule from each sampled interval was assayed, to exclude the possibility of mixing non-coeval carbonates. For 'dirty' calcites, the preferred method for generating isochron data points is to leach or totally dissolve samples containing differing amounts of detrital contaminant to provide a range of isotopic compositions sufficient to define the required mixing line. This approach was unsuitable here because the homogenous distribution of detritus throughout the nodule limits the data spread. Instead a strategy similar to that of Ku and Liang (1984) was adopted, in which the required data spread is generated by leaching homogenous subsamples in dilute acids of differing molarities and by total sample dissolution (Appendix).

5.2. Stable isotopes

To verify that our dated nodules are isotopically typical of the numerous nodules previously discussed in the literature, we analysed their carbon and oxygen isotopic compositions. Two samples from each pulverised nodule were reacted with 100% phosphoric acid and the CO_2 isotopic composition measured on a VG Sira Series II mass spectrometer, calibrated using NBS 19 and NBS 18 standards. Oxygen and carbon isotopic ratios are reported in the standard delta notation relative to the Vienna Pee Dee Belemnite (VPDB) international scale.

6. Results

6.1. Uranium-series dating

The measured isotopic compositions of the samples are shown in Table 1 and the isotopic ratios in Table 2. Isochron-derived authigenic $^{230}Th/^{234}U$ and $^{234}U/^{238}U$ values and calculated ages are summarised in Table 3 and the data shown graphically in Fig. 4. For illustrative purposes, the plots are shown in two dimensions and the regression lines shown were fitted using the algorithm of York (1969). (For these particular samples, the calculated isochrons and ages obtained using the three-dimensional procedure of Ludwig (1994) are insignificantly different from those obtained using York's algorithm).

The U/Th data for the calcrete nodules from below palaeosol S_1 at Luochuan and below the lower palaeosol (at ~ 6 m depth) at Liujiapo display good linearity. The mean square of weighted deviates (MSWD) values, a measure of observed data scatter relative to the scatter predicted from

Table 1
Carbonate nodule analytical and isotopic data[a]

Lab. sample No.	Acid used	Insol. (%)	U (ppm)	Yield (%)		Specific activity (dpm g^{-1})			
				U	Th	238-U	234-U	232-Th	230-Th
Liujiapo (upper nodule) ~2.7 m depth									
UEA612	0.5N	37	0.44	32	3	0.331 (7)	0.388 (8)	0.414 (10)	0.370 (9)
UEA618	0.5A	38	0.46	32	14	0.341 (8)	0.376 (8)	0.395 (9)	0.351
UEA621	TSD	0	1.36	36	19	1.012 (22)	1.015 (22)	0.567 (19)	0.375 (15)
Liujiapo (lower nodule) ~6 m depth									
UEA611	0.5N	41	2.10	40	5	1.572 (16)	1.891 (18)	0.377 (9)	0.477 (10)
UEA602	0.1N	41	1.83	48	11	1.365 (27)	1.630 (29)	0.323 (12)	0.448 (14)
UEA617	0.5A	43	1.66	25	19	1.240 (25)	1.586 (29)	0.238 (11)	0.393 (14)
UEA622	TSD	0	2.88	40	27	2.156 (44)	2.567 (48)	1.487 (40)	1.116 (35)
Luochuan (base S_1)									
UEA603	0.5N	42	0.54	55	12	0.406 (6)	0.504 (7)	0.407 (7)	0.377(7)
UEA609	0.1N	42	0.55	36	39	0.414 (9)	0.514 (10)	0.390 (8)	0.374 (7)
UEA610	1.0A	43	0.53	4	39	0.397 (11)	0.554 (13)	0.341 (8)	0.351(8)
UEA614	0.5A	43	0.50	11	45	0.373 (9)	0.504 (10)	0.335 (9)	0.346 (9)
UEA623	TSD	0	1.59	36	23	1.186 (23)	1.195 (24)	1.321 (34)	0.978 (29)
Luochuan (base S_{2-1})									
UEA625	TSD	0	1.61	65	28	1.202 (24)	1.302 (24)	1.629 (42)	1.405 (39)
UEA627	1.0A	48	0.57	6	21	0.428 (11)	0.551 (12)	0.377 (7)	0.541 (9)
UEA637	0.2N	45	0.61	35	12	0.455 (10)	0.534 (11)	0.435 (10)	0.511 (11)
UEA753[b]	TSD	0	2.08	73	19	1.553 (44)	1.312 (40)	2.913 (118)	2.169 (101)
UEA761	0.1N	42	0.63	85	59	0.472 (14)	0.579 (16)	0.443 (15)	0.495 (16)
Luochuan (base S_{2-2})									
UEA626	TSD	0	2.13	48	5	1.588 (29)	1.655 (30)	1.743 (40)	1.346 (36)
UEA628	1.0A	61	0.70	16	17	0.525 (11)	0.659 (12)	0.493 (10)	0.586 (11)
UEA638	0.2N	56	0.74	25	11	0.551 (11)	0.730 (12)	0.621 (13)	0.623 (13)
UEA640	0.2N	58	0.74	39	27	0.554 (14)	0.734 (17)	0.615 (15)	0.588 (15)

[a] The errors are shown in parentheses and refer to last decimal place(s), they represent 1 S.D. (counting statistics only); the acids used for sample leaching are nitric (N) and acetic (A);TSD total sample dissolution using $HNO_3/HClO_4/HF$ and numbers refer to molarity of the acid.
[b] Residue of UEA637.

analytical errors (Wendt and Carl, 1991), are close to unity, at 0.54 for the Luochuan nodule and 1.73 for the Liujiapo nodule. The MSWD value will be close to 1 when the observed variations about the regression plane are within analytical error and there is no additional (geological) scatter due to heterogenous samples. Thus, these values suggest that the data scatter for the Luochuan sample derives from assigned measurement errors but that some additional geological scatter is present in the Liujiapo data.

For the nodule from below palaeosol S_1 at Luochuan, the calculated age (if all the data are considered) is 62 ± 21 ka (95% confidence). However, one data point (UEA610) can be seen to lie below the linear trend defined by the other four points (Fig. 4). This probably indicates preferential leaching of ^{232}Th relative to ^{230}Th compared with the other samples. If this deviant point is omitted, the calculated age of the nodule is 71 ± 27 ka. At the 95% confidence level, these ages fall between mid-oxygen isotope stage 3 and oxygen isotope stage 5c (~45–99 ka).

For the nodule from below the lower palaeosol (~6 m depth) at Liujiapo, the U/Th data give an age of 21.2 ± 5.7 ka (95% confidence), that is,

Table 2
Carbonate nodule U-series isotopic ratios

Lab. sample No.	234-U/238-U	230-Th/234-U	238-U/232-Th	234-U/232-Th	230-Th/232-Th
Liujiapo (upper nodule)					
UEA612	1.171 (35)	0.953 (43)	0.801 (36)	0.937 (42)	0.894 (31)
UEA618	1.102 (34)	0.935 (41)	0.863 (38)	0.951 (41)	0.889 (28)
UEA621	1.002 (31)	0.370 (20)	1.784 (85)	1.788 (85)	0.661 (35)
Liujiapo (lower nodule)					
UEA602	1.203 (17)	0.252 (13)	4.164 (214)	5.010 (257)	1.264 (41)
UEA611	1.194 (32)	0.275 (12)	4.231 (208)	5.053 (246)	1.388 (68)
UEA617	1.279 (35)	0.247 (12)	5.218 (296)	6.674 (373)	1.652 (96)
UEA622	1.190 (33)	0.435 (19)	1.450 (60)	1.726 (70)	0.750 (31)
Luochuan (base S_1)					
UEA603	1.240 (24)	0.749 (30)	0.997 (40)	1.236 (49)	0.926 (24)
UEA609	1.241 (35)	0.727 (31)	1.062 (45)	1.317 (55)	0.958 (27)
UEA610	1.394 (50)	0.634 (31)	1.164 (60)	1.623 (87)	1.029 (33)
UEA614	1.348 (41)	0.687 (30)	1.116 (51)	1.505 (67)	1.034 (39)
UEA623	1.008 (28)	0.818 (40)	0.897 (41)	0.905 (42)	0.740 (29)
Luochuan (base S_{2-1})					
UEA625	1.083 (29)	1.079 (53)	0.738 (36)	0.799 (39)	0.863 (32)
UEA627	1.287 (43)	0.983 (48)	1.136 (59)	1.462 (74)	1.438 (37)
UEA637	1.174 (34)	0.957 (47)	1.046 (53)	1.228 (62)	1.175 (38)
UEA753	0.845 (32)	1.653 (97)	0.533 (28)	0.450 (24)	0.745 (44)
UEA761	1.227 (45)	0.854 (46)	1.065 (60)	1.308 (72)	1.117 (49)
Luochuan (base S_{2-2})					
UEA626	1.042 (27)	0.814 (39)	0.911 (43)	0.949 (44)	0.772 (27)
UEA628	1.256 (35)	0.888 (45)	1.066 (55)	1.338 (68)	1.189 (34)
UEA638	1.324 (34)	0.853 (42)	0.888 (44)	1.176 (58)	1.003 (29)
UEA640	1.326 (34)	0.801 (35)	0.901 (40)	1.195 (52)	0.957 (26)

Table 3
Isochron-derived authigenic U-series isotopic ratios, resultant calculated ages and correlated marine oxygen isotope stage[a]

Sample	230-Th/ 234-U	234-U/ 238-U	Probability of fit	Calculated age (ka)	Oxygen isotope stage
Liujiapo (lower nodule, ~6 m depth)	0.178 ± 0.041	1.237 ± 0.108	0.14	21.2 ± 5.7	2
Luochuan (base S_1)	0.458 ± 0.119 (0.508 ± 0.142)	2.689 ± 0.905 (2.728 ± 1.080)	0.78 (0.91)	62.0 ± 21 (71.0 ± 27)	3–5c

[a] Ages and errors have been calculated using the Isoplot program of Ludwig (1994), which utilises the three-dimensional isochron algorithms developed in Ludwig and Titterington (1994). Errors are 95% confidence limits Numbers in parentheses exclude data point UEA610.

within oxygen isotope stage 2. These data indicate that the nodules have formed *not* during full interglacial periods but during interstadial, stadial or transitional stages.

The data for the nodules from below S_{2-1} and S_{2-2} at Luochuan displayed considerable scatter with MSWD values >3. This scatter probably reflects either geological inhomogeneity in the samples or differential isotopic fractionation, especially ^{230}Th fractionation, between samples during leaching. Consequently, the isochrons are unreliable. Preliminary analysis of the nodule from below the upper palaeosol (~2.75 to 0.5 m depth) in the Liujiapo sequence revealed a negatively

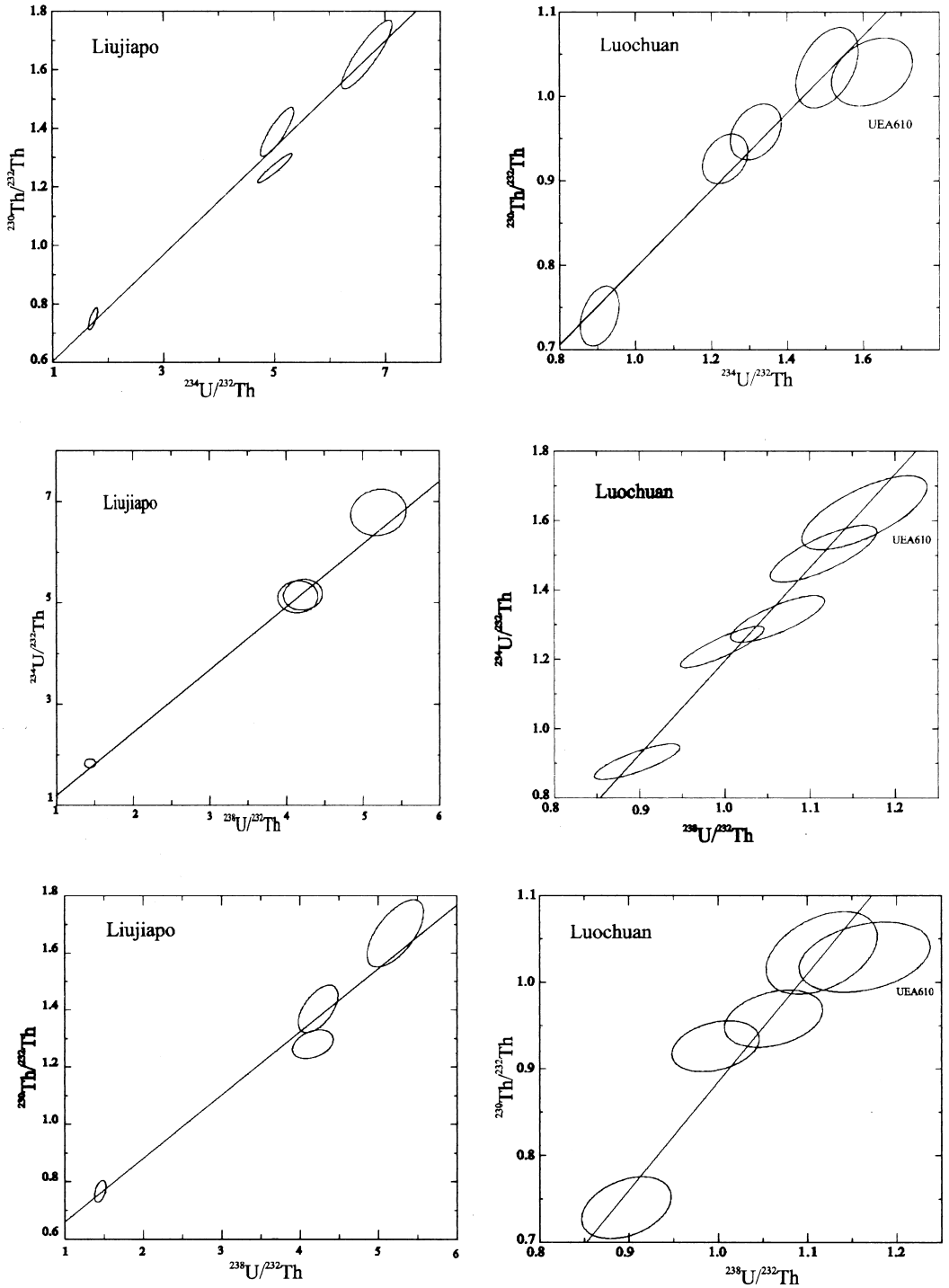

Fig. 4. Isochron plots of the Liujiapo and Luochuan U-series data projected onto the three planes which bound the three-dimensional space containing the fitted maximum-likelihood (MLE) regression line (Ludwig and Titterington, 1994). The regression lines shown have been fitted by the least squares method of York (1969) which in this case gives results very similar to the MLE method (Table 3). MSWD for Liujiapo and Luochuan are 1.73 and 0.544, respectively.

Table 4
Carbon and oxygen isotope data and estimated $\delta^{18}O_{VSMOW}$ values for palaeoprecipitation (see text); $\delta^{18}O$ of modern meteoric water at Luochuan is 9.6‰ $_{VSMOW}$; and modern average annual precipitation at Liujiapo is −7.10‰ $_{VSMOW}$

Sample	$\delta^{13}C_{CaCO_3}$ (‰ $_{VPDB}$)	$\delta^{18}O_{CaCO_3}$ (‰ $_{VPDB}$)	δ^{18}Oprecip (‰ $_{VSMOW}$)
Liujiapo (upper nodule, ~ 2.75 m depth)	−6.824 + 0.004	−9.127 + 0.007	−10.1
	−6.801 + 0.003	−9.127 + 0.014	
Liujiapo (lower nodule, ~6 m depth)	−7.553 + 0.004	−8.585 + 0.005	−9.6
	−7.535 + 0.003	−8.604 + 0.006	
Luochuan (base S_1)	−5.651 + 0.004	−9.272 + 0.003	−10.3
	−5.635 + 0.007	−9.324 + 0.009	
Luochuan (base S_{2-1})	−3.592 + 0.003	−9.686 + 0.004	−10.5
	−3.578 + 0.007	−9.475 + 0.010	
Luochuan (base S_{2-2})	−4.863 + 0.004	−9.201 + 0.010	−10.2
	−4.776 + 0.006	−9.147 + 0.006	

sloping 'isochron', indicating severe differential isotopic fractionation. This sample was not investigated further.

Ludwig (1994) has pointed out that the uncertainties of isochron ages derived from three or four data points can be significantly greater than calculated by regression algorithms because there is a possibility of obtaining highly linear plots by chance. In both the cases under consideration here, a total sample dissolution (TSD) data point is conformable with the observed leachate trend. This strongly suggests that differential isotopic fractionation during leaching has been negligible; therefore, the leachate data represent a true mixing line and the observed linearity is not due to a chance alignment. It may be noted also that Kaufman et al. (1992) present several three- or four-point leachate plots from Dead Sea lacustrine deposits that give presumed accurate ages in correct stratigraphic order.

Whilst this rigorous treatment of the data gives us confidence in the U-series dates, some caution is due because:

1. the nodules may have formed over a period of a few thousand years;
2. only individual nodules from each horizon have so far been dated; and
3. the 95% confidence age errors are ~25% for the Liujiapo nodule and ~33% for the Luochuan nodules.

It should be noted, however, these age errors notwithstanding, neither date is compatible with nodule formation during an interglacial stage.

6.2. Carbon and oxygen isotopes

The stable isotope results from the sampled Luochuan and Liujiapo nodules (both dated and undated) are shown in Table 4 and plotted in Fig. 5. The isotopic values are very similar to those reported for numerous nodules beneath palaeosols S_1 to S_{14} at Luochuan by Han et al. (1997), Wang and Zheng (1989) and Zheng et al. (1987). $\delta^{13}C$ values lie mainly in the range −4 to −8‰$_{PDB}$ and $\delta^{18}O$ between −8.6 and −10.2‰$_{PDB}$. Our $\delta^{13}C$ value from the Luochuan S_1 nodule is slightly enriched, at −3.5‰, and that of Han et al. (1997) from the same horizon is even more enriched (−2.59‰). It is notable that all the available data for the Chinese Loess Plateau display a linear and negative relationship between oxygen and carbon isotopic values (Fig. 5). This relationship suggests that the isotopic contribution of detrital (isotopically-enriched) carbonate occur is negligible. It also indicates that kinetic effects, such as evaporation, are probably unimportant and isotopic equilibrium between seepage water and calcite may have been maintained during calcite precipitation.

7. Discussion

7.1. Comparison of the nodule U-series ages with published age data

The isotopic data suggest that the nodules investigated here are typical of the nodule populations from which they were sampled. The two U-series dates indicate formation of the sampled nodules during glacial or transitional climate stages rather than during interglacial periods. The date of 21.2 ± 5.7 ka for the nodule below the lower palaeosol ($\sim$6 m depth) at Liujiapo is consistent with published ^{14}C dates obtained from pedogenic carbonates from sites across the Loess Plateau, often from depths of 4–6 m (Pye and Zhou, 1989 and references therein). These ^{14}C dates range between 21.4 and 24.5 ka. They can be considered as minimum ages since they may contain younger soil-derived CO_2 and also have not been corrected for past fluctuations in ^{14}C production (Bard et al., 1990). Nevertheless, they indicate pedogenic carbonate formation across the Loess Plateau during either oxygen isotope stage 2 or late stage 3 since their stratigraphic depth precludes much older ages.

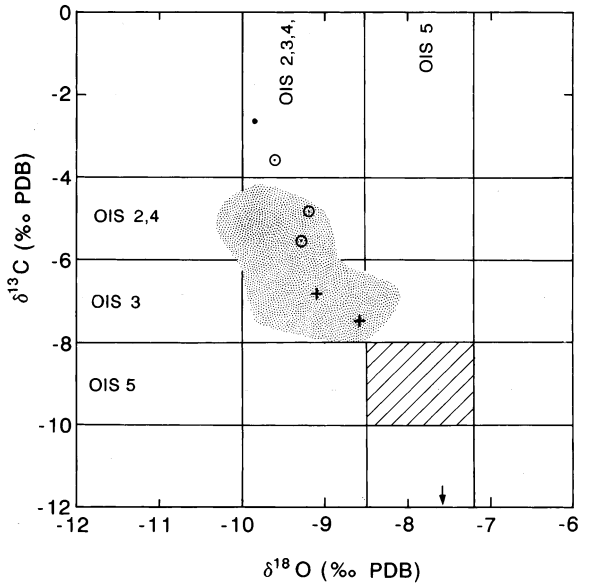

Fig. 5. $\delta^{13}C$ versus $\delta^{18}O$ plot for calcrete nodules and carbonate cements from the Chinese Loess Plateau. The stippled area defines the range of published data from Luochuan (Han et al., 1997; Wang and Zheng, 1989; and Zheng et al., 1987). ● data point for nodule from beneath palaeosol S_{2-1} (Han et al., 1997); ⊙, Luochuan nodule data (this study, Table 4); + Liujiapo nodule data (this study, Table 4). Arrow indicates the expected $\delta^{18}O$ value of carbonate precipitating in isotopic equilibrium with meteoric water at Luochuan today. 'OIS 2, 3, 4, 5' identify boxes defining the isotopic ranges recorded for secondary carbonate cements from the Loess Plateau for oxygen isotope stages 2–5; the diagonally shaded box indicates the isotopic composition of carbonate cements formed during the last interglacial (Lin et al., 1991; Wang et al., 1997).

The combination of published TL dates from the upper $\sim$5.5 m of the Liujiapo sequence (Musson et al., 1994) and our U-series age for the nodule from the lower palaeosol ($\sim$6 m) allows closer examination both of the higher-resolution variability of climate and of the chronostratigraphic relationship between soils and nodules. Fig. 3(a and b) indicate that soil formation proceeded during the first half of oxygen isotope stage 3. Deposition of loess subsequently prevailed, almost until the end of oxygen isotope stage 2, when weak palaeosol development restarted. These changes are reflected in the magnetic susceptibility signal [Fig. 3(a)] and the accumulation rate [Fig. 3(b)]. Fig. 3 indicates that our dated nodule ($\sim$21 ka) formed $\sim$5 m below the contemporary land surface. The nodule thus post-dates the palaeosol below which it lies by $\sim$40 kyr. This identifies injection of carbonate into the older palaeosol from the overlying interstadial soil and loess. Therefore, calcrete nodules cannot be assumed to be directly related (geochemically, isotopically or genetically) to the soil beneath which they immediately lie.

The U-series ages for the nodule below S_1 at Luochuan, of 62 ± 21 ka or 71 ± 27 ka, indicate its formation during late stage 5, stage 4 or early stage 3. In comparison, matching of the magnetic susceptibility record of the sequence at nearby Xifeng (35.7°N 107.6°E) with the deep-sea oxygen isotope record (Bloemendal et al., 1995; Thompson and Maher, 1995) indicates a stage 5e age for S_1. Again, the U-series ages suggest that the nodule post-dates the soil beneath which it lies or, alternatively, formed at an extremely late stage in the development of that soil.

The formation of calcrete nodules depends inter alia on the presence of sufficient precipitation to

leach carbonate from the near-surface but insufficient to remove it in solution from the system before supersaturation can occur. The U-series dates suggest that conditions favouring nodule formation occurred preferentially at, or subsequent to, the warm stage/cold stage transition.

7.2. Comparison of the nodule isotopic data with published data

In previous studies of the stable isotope compositions of calcrete nodules in the Chinese loess-palaeosol sequences (Han et al., 1997; Zheng et al., 1987), it has been assumed that the isotopic composition of the nodules found below any individual palaeosol relates directly to the period of time when *that* palaeosol was forming. On this basis, Han et al. (1997) first assign maximum and minimum palaeotemperature and rainfall values to the 'most-developed' and 'least developed' palaeosols, S_{5-2} and S_{2-1}, respectively (14°C and 800 mm rain a^{-1} for S_{5-2} and 10°C and 500 mm rain a^{-1} for S_{2-1}). The isotopic data from the underlying calcrete nodules are then used to interpolate from these assigned values and estimate temperature and rainfall values for the remaining palaeosols. However, given the U-series evidence of a diachronous relationship between palaeosols and underlying nodules, palaeoclimatic information derived from the isotopic composition of the nodules will relate to conditions at the time of nodule (rather than palaeosol) formation.

For Luochuan and Duanjiapo, near Xi'an, Lin et al. (1991) have published stable isotope profiles from palaeosol S_1 to the present day, through partially cemented loess/palaeosol sections. Wang et al. (1997) have published similar data for Liujiapo. Frakes and Sun (1994) have constructed a $\delta^{13}C$ record, from secondary calcite cement, for the past 180 ka from Luochuan. Potential problems with such records are that:

1. it is difficult to correct accurately the isotopic data for any detrital (isotopically enriched) carbonate contribution (likely to be a particular problem in the loess units); and
2. the chronological relationship of the secondary carbonate cement to the sedimentary stratigraphy is unknown.

Nevertheless, the records appear to show marked differences between the isotopic signatures associated with palaeosol formation and those associated with loess accumulation. Broadly, for Luochuan, $\delta^{13}C$ values during glacial stages (oxygen isotope stages 2 and 6) lie in the range -4 to $-6‰_{PDB}$ whilst during interglacials (oxygen isotope stages 1 and 5), lighter values of -8 to $-10‰$ are more typical. During oxygen isotope stages 3 and 4, $\delta^{13}C$ values ranged between -6 and $-8‰_{PDB}$. For Duanjiapo, a similar overall pattern is seen, although $\delta^{13}C$ values are generally 1–2‰ lighter than at Luochuan. $\delta^{18}O$ values show less variation; interglacial values lie between -7 and $-8.5‰_{PDB}$ whilst for other time periods the range is -8.5 to $-10‰$. In Fig. 5, our nodule data are compared with those of Han et al. (1997), Wang and Zheng (1989) and Zheng et al. (1987), all from Luochuan, in $\delta^{13}C$ versus $\delta^{18}O$ space. It can be seen that the $\delta^{13}C$ values for the nodules (-2.5 to $-7.8‰_{PDB}$) are significantly heavier than those recorded from secondary cements for both the last interglacial period (130 to 70 ka) and the Holocene. Conversely, they closely match the data for the glacial stage periods, 185 to 130 and 70 to 10 ka (-4 to $-8‰_{PDB}$). Similarly, the observed $\delta^{18}O$ values of the nodules (-8.2 to $-10.2‰_{PDB}$) fall mainly into the 'glacial' range of Lin et al. (1991) rather than their interglacial range (-7.2 to $-8.5‰$).

7.3. Palaeoclimatic implications

The depth of the nodules makes it unlikely that their relatively enriched carbon values reflect an atmospheric contribution. The more likely interpretation is that they result from a reduced proportion of C_3 plants in the biomass, possibly reflecting levels of water stress above those observed today. Frakes and Sun (1994) suggest that the proportion of C_3 biomass during episodes of soil formation varied from ca. 65 to 80% whereas between these episodes 55–60% was more typical.

The $\delta^{13}C$ data thus independently support the U-series data by suggesting that nodule formation occurred under less humid, cold stage conditions, when the C_3 contribution to the carbon signal was significantly reduced. The date for the Luochuan

nodule (~71 ka) suggests it formed at around the oxygen isotope stage 5/4 boundary. Although the age errors are large, they are not compatible with nodule growth at the height of the last interglacial (i.e. oxygen isotope stage 5e). The *relative* increase in C_4 vegetation inferred from the $\delta^{13}C$ data suggests that although conditions may have become drier following the end of full interglacial conditions, summer temperatures on the central Loess Plateau may not have been much cooler than the present day, given the preference of C_4 species for high temperatures during the summer months (Teeri and Stowe, 1976; Caldwell et al., 1977; Hattersley, 1983). An additional factor that may affect the C_4 component is the change in atmospheric pCO_2 during glacial and interglacial periods (Cerling et al., 1997; Ehleringer et al., 1997); C_4 plants are favoured by low atmospheric pCO_2.

Given the strong correlation between the $\delta^{18}O$ compositions of modern soil carbonates and local meteoric water demonstrated by Cerling (1984) and Cerling and Quade (1993), it is possible to fit regression equations to their data and thence derive meteoric water values from other sets of carbonate oxygen data, such as those from the Loess Plateau. However, the considerable data scatter about the fitted regression lines makes such a step rather hazardous. This is especially so since the temperature at which the carbonate is precipitated has a significant effect on its $\delta^{18}O$ value and little is known at present about seasonal or diurnal bias in the formation of modern or Pleistocene pedogenic carbonates. Fig. 6 shows the relationship between temperature, $\delta^{18}O$(water) and $\delta^{18}O$(carbonate) for calcite precipitating in isotopic equilibrium with its parent water (O'Neil et al., 1969). The range of oxygen isotope data for the carbonates from the Loess Plateau is also shown. It is evident that these carbonate isotopic compositions could be produced by a wide range of meteoric water compositions and soil temperatures. At Xi'an, the average $\delta^{18}O$ value of precipitation from 1985 to 1987 was $-7.12‰_{VSMOW}$ and the average annual temperature was 13.9°C (Rozanski et al., 1993). At Luochuan, groundwater values are reported to be $-9.6‰_{VSMOW}$ (Zheng et al., 1987) and the average annual temperature 9.2°C (Han et al., 1997). Carbonate precipitating in isotopic equilibrium today might thus be expected to have $\delta^{18}O$ values of ca. $-6.4‰_{PDB}$ at Liujiapo and ca. $-7.8‰_{PDB}$ at Luochuan. These values are significantly more enriched than those observed for our Pleistocene nodules. Conversely, Lin et al.'s (1991) data for interglacial stage carbonate cements from Luochuan, with $\delta^{18}O$ values typically -8.2 to $-7.2‰_{PDB}$, *are* compatible with formation close to equilibrium with present meteoric waters at the modern average annual temperature (although other combinations of temperature–water $\delta^{18}O$ are also possible). Soil carbonate data from Liujiapo (Wang et al., 1997) also indicate that last interglacial $\delta^{18}O$ values, lying in the range -6.0 to $-7.2‰_{PDB}$, are more enriched than those observed for the nodules. The negative correlation between the $\delta^{18}O$ and $\delta^{13}C$ values, and the fact that none of the nodules display $\delta^{18}O$ values more enriched than those compatible with equilibrium deposition from modern meteoric water, suggest that kinetic fractionation has not significantly influenced the nodule isotopic compositions.

We can identify the possible formation conditions of the nodules by examining the relationship of the modern temperature–meteoric water data with the isotopic composition of the Pleistocene nodules. For example, Fig. 6 shows the modern temperature and meteoric water $\delta^{18}O$ data (point A) and the isotopic datum for our sampled nodule underlying palaeosol S_1 at Luochuan (the horizontal dashed line at $-9.3‰_{PDB}$). The nodule composition could be produced by:

1. the nodule formation temperature being ~6° C warmer than present at Luochuan (A–B in Fig. 6), with the isotopic composition of precipitation being similar to the modern value; or
2. the formation temperature being >6° C warmer and the meteoric water enriched relative to the present day (A–B–C on Fig. 6); or
3. formation temperature being 0–6°C warmer than today and precipitation isotopically more depleted by up to $1.5‰_{VSMOW}$ (A–B–D on Fig. 6); or
4. formation temperatures being cooler than at present and precipitation being isotopically more depleted by >1.5‰ (A–D–E on Fig. 6).

Similar considerations apply to the Liujiapo data,

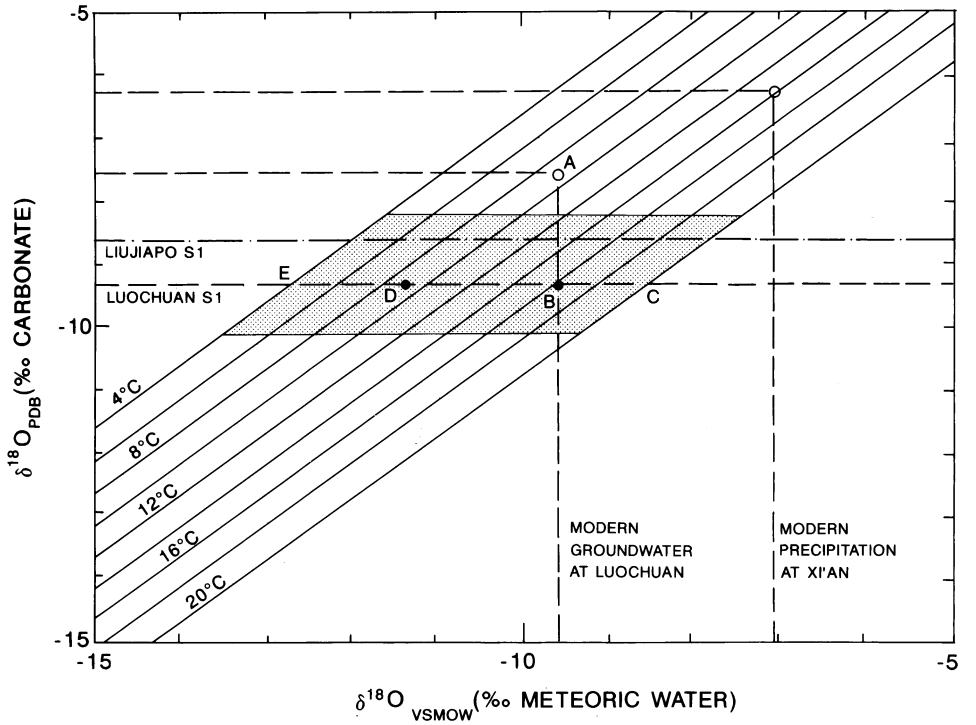

Fig. 6. Relationship between temperature, $\delta^{18}O_{water}$ and $\delta^{18}O_{carbonate}$ for calcium carbonate precipitating in isotopic equilibrium (O'Neil et al., 1969). The stippled area represents the range of $\delta^{18}O_{carbonate}$ values recorded for nodules from the Loess Plateau (this study, Han et al., 1997; Wang and Zheng, 1989; and Zheng et al., 1987). Labelled horizontal lines refer to the $\delta^{18}O_{carbonate}$ values of the nodules dated here (Table 4). See text for explanation of A–E.

also shown in Fig. 6. The U-series dates from Luochuan and Liujiapo suggest that explanation (4) is most likely to describe the climatic conditions at the time of nodule formation. This interpretation is supported by two independent lines of evidence. First, the nodule isotopic compositions accord with isotopic data from cold-stage sections of the published loess/palaeosol profiles (Lin et al., 1991; Frakes and Sun, 1994; Wang et al., 1997). Second, as shown in Fig. 3, nodule formation at Liujiapo (at 21 ka) coincides with moderately low values of pedogenic magnetic susceptibility, indicating reduced rainfall (Heller et al., 1993; Maher et al., 1994). This implies a weakened summer monsoon, one result of which would be isotopically more depleted precipitation toward the continental interior (Rozanski et al., 1993). Han et al. (1997), using a regression equation derived from Cerling's (1984) data, also concluded that palaeoprecipitation would have been isotopically more depleted, but assuming the nodules relate to interglacial (soil-forming) climate stages, they then estimated that palaeotemperatures would have been higher than today by 0.5–4.5° C.

There may be some similarities between the pattern of climatic and hydrological changes in the Chinese Loess Plateau and that inferred by Ayliffe et al. (1998) in southeastern Australia. Their speleothem studies suggest that stadials and cool interstadials were the times of highest effective precipitation (leading to abundant speleothem growth), whilst interglacials represent periods of high evaporation resulting in a net water deficit and very little calcite precipitation.

In summary, the observed negative relationship for the calcrete nodules — enriched $\delta^{13}C$ values associating with depleted $\delta^{18}O$ values — is consistent with carbonate precipitation at times of weakened summer monsoon and/or reduced atmospheric pCO_2 levels.

8. Conclusions

1. U-series isochron dates from calcrete nodules in the Chinese loess and palaeosol sequences show that a nodule underlying palaeosol S_1 at Luochuan formed sometime between late oxygen isotope stage 5 and stage 3, and that a nodule underlying an upper palaeosol ($\sim$6 m depth) at Liujiapo formed during oxygen isotope stage 2.
2. The U-series date for the Liujiapo nodule, taken in conjunction with published luminescence ages for this sequence, indicates that the nodule post-dates by $\sim$40 kyr the palaeosol below which it immediately lies. Therefore, carbonate must have been injected into the older palaeosol from the overlying interstadial soil and loess. Thus, calcrete nodules cannot be assumed to be directly related (geochemically, isotopically or genetically) to the soil beneath which they immediately lie.
3. Stable isotope analyses of the calcrete nodules provide independent support for their formation during globally cooler (non-interglacial) climate stages. The carbon isotopic values probably reflect a decreased proportion of C_3 plants, implying increased levels of water stress and/or reduced atmospheric pCO_2 levels. The oxygen data suggest that meteoric water at the time of carbonate precipitation was isotopically lighter than at present, implying a weakened summer monsoon.

Acknowledgements

The authors are very grateful to Professor Sun, Xi'an College of Geology, for help during fieldwork and sample collection in China, Dr Zhou Li Ping, The McDonald Institute for Archaeological Research, University of Cambridge for assistance in the field and for magnetic susceptibility measurements and Dr Julian Andrews for assistance with microscopy. Phillip Judge drew the figures. This work was supported in part by a research grant from the University of East Anglia.

Appendix:Preparation of samples for U series assay

Sub-samples of the pulverised nodules were leached in an excess of dilute nitric acid (typically 0.1 or 0.2M) or acetic acid (1.0 or 0.5M). A $^{229}Th/^{236}U$ spike, calibrated against a uraninite standard, was added to the leachate solution and allowed to equilibrate prior to the addition of the sample in small aliquots. Very dilute acids were used in order to maximise data spread and minimise isotopic fractionation between samples. They also minimised the amount of silica leached from the samples. To provide data proximal to the detrital end-member, sub-samples were totally dissolved in $HF/HClO_4/HNO_3$. Uranium and thorium isotopes were concentrated by $Fe(OH)_3$ precipitation and separation and purification was on anion exchange columns in hydrochloric and nitric acid media, respectively. The isotopes were finally electroplated onto stainless steel discs from an ammonium sulphate solution. Counting was on E.G.&G. Ortec surface barrier detectors and FWHM resolution was 35–40 keV.

References

Ayliffe, L.K., Marienelli, P.C., Moriaty, K.C., Wells, R.T., McCulloch, M.F., Mortimer, G.E., Hellstrom, J.C., 1998. 500 ka precipitation record from southeastern Australia: evidence for interglacial relative aridity. Geology 26, 147–150.

Bard, E., Hamelin, B., Fairbanks, R.G., Zindler, A., 1990. Calibration of the 14C timescale over the past 30,000 years using mass spectrometric U–Th ages from Barbados corals. Nature 345, 405–410.

Bischoff, J.L., Fitzpatrick, J.A., 1991. U-series dating of impure carbonates: an evaluation of the isochron technique using total sample dissolution. Geochim. Cosmochim. Acta 55, 543–554.

Bischoff, J.L., Julia, R., Mora, R., 1988. Uranium-series dating of the Mousterian occupation at Abric Romani, Spain. Nature 332, 68–70.

Bloemendal, J., Liu, X.M., Rolph, T.C., 1995. Correlation of the magnetic susceptibility stratigraphy of Chinese loess and the marine oxygen-isotope record — chronological and paleoclimatic implications. Earth Planet. Sci. Lett. 131, 371–380.

Caldwell, M.M., White, R.S., Moore, R.T., Camp, L.B., 1977. Carbon balance, productivity and water use of cold-winter

desert shrub communities dominated by C3 and C4 species. Oecologia 29, 275–300.
Cerling, T.E., 1984. The stable isotopic composition of modern soil carbonate and its relationship to climate. Earth Planet. Sci. Lett. 71, 229–240.
Cerling, T.E., Quade, J., 1993. Stable carbon and oxygen isotopes in soil carbonates. In: Swart, P.K., Lohmann, K.C., McKenzie, J., Savin, S. (Eds.), Climate changes in Continental Isotopic Records, Am. Geophys. Union Geophys. Monogr. 78, 217–231.
Cerling, T.E., Harris, J.M., MacFadden, B.J., Leakey, M.J., Quade, J., Eisenmann, V., Ehleringer, J.R., 1997. Global vegetation change through the Miocene/Pliocene boundary. Nature 389, 153–158.
Chen, F.H., Bloemendal, J., Wang, J.M., Li, J.J., Oldfield, F., 1997. High-resolution multi-proxy climate records from Chinese loess: evidence for rapid climatic changes over the last 75 kyr. Palaeogeogr., Palaeoclimatol., Palaeoecol. 130, 323–335.
Deines, P., 1980. The isotopic composition of reduced organic carbon. In: Fritz, P., Frontes, J.C. (Eds.), Handbook of Environmental Geochemistry vol. 1. Elsevier, Amsterdam, pp. 329–406.
Ehleringer, J.R., Cerling, T.E., Helliker, B.R., 1997. C-4 photosynthesis, atmospheric CO2 and climate. Oecologia 112, 285–299.
Frakes, L.A., Sun, J., 1994. A carbon isotope record of the upper Chinese loess sequence: estimates of plant types during stadials and interstadials. Palaeogeogr., Palaeoclimatol., Palaeoecol. 108, 183–189.
Gu, Z., Liu, R., Liu, Y., 1991. Response of the stable isotopic composition of loess-palaeosol carbonate to palaeoenvironmental changes. In: Liu, T.S. (Ed.), Loess Environment and Global Change. Science Press, Beijing, pp. 82–92.
Han, J., Keppens, E., Liu, T., Paepe, R., Jiang, W., 1997. Stable isotope composition of the calcrete nodule in loess and climate change. Quat. Int. 37, 37–43.
Hattersley, P.W., 1983. The distribution of C3 and C4 grasses in Australia in relation to climate. Oecologia 57, 113–128.
Heller, F., Shen, C.D., Beer, J., Liu, X.M., Liu, T.S., Bronger, A., Suter, M., Bonani, G., 1993. Quantitative estimates and palaeoclimatic implications of pedogenic ferromagnetic mineral formation in Chinese loess. Earth Planet. Sci. Lett. 114, 385–390.
Ivanovich, M., Harmon, R.S. (Eds.), Uranium-series Disequilibrium: Applications to Earth Marine and Environmental Sciences 1992. Clarendon Press, Oxford, pp. 779–781.
Kaufman, A., 1971. U-series dating of Dead Sea basin carbonates. Geochim Cosmochim. Acta 35, 1269–1281.
Kaufman, A., 1991. An evaluation of several methods for determining 230Th/U ages in impure carbonates. Geochim. Cosmochim. Acta 57, 2303–2317.
Kaufman, A., Yechieli, Y., Gardosh, M., 1992. Reevaluation of the lake-sediment chronology in the Dead Sea basin Israel based on new 230Th/U dates. Quat. Res. 38, 292–304.
Ku, T.L., Liang, Z.C., 1984. The dating of impure carbonates with decay series isotopes. Nucl. Instrum. Meth. 223, 563–571.
Ku, T.L., Bull, W.E., Freeman, S.T., Knauss, K.G., 1979. 230Th/234U dating of pedogenic carbonates in gravelly deserts of Vidal Valley Southwestern California. Bull. Geol. Soc. Am. 90, 1063–1073.
Langmuir, D., Herman, J.S., 1980. The mobility of thorium in natural waters at low temperatures. Geochim. Cosmochim. Acta 44, 1753–1766.
Latham, A.G., Schwarcz, H.P., 1992. Carbonate and sulphate precipitates. In: Ivanovich, M., Harmon, R.S. (Eds.), Uranium-series Disequilibrium: Applications to Earth Marine and Environmental Sciences. Clarendon Press, Oxford, pp. 423–459.
Lin, B., Liu, R., An, Z., 1991. Preliminary research on stable isotopic compositions of Chinese loess. In: Liu, T.S.et al., (Eds.), Loess Environment and Global Change. Science Press, Beijing, pp. 124–131.
Luo, S., Ku, T.-L., 1991. U-series isochron dating: a generalised method employing total sample dissolution. Geochim. Cosmochim. Acta 55, 555–564.
Ludwig, K.R., 1994. ISOPLOT — a plotting and regression program for radiogenic-isotope data. Version 2.75. Revision of U.S.G.S. Open-File Report 91-445.
Ludwig, K.R., Titterington, D.M., 1994. Calculation of 230Th/U isochrons, ages and errors. Geochim. Cosmochim. Acta 58, 5031–5042.
Maher, B.A., 1998. Magnetic properties of modern soils and loessic paleosols: implications for paleoclimate. Palaeogeogr. Palaeoclimatol., Palaeoecol. 137, 25–54.
Maher, B.A., Thompson, R., Zhou, L.P., 1994. Spatial and temporal reconstructions of changes in the Asian palaeomonsoon: a new mineral magnetic approach. Earth Planet. Sci. Lett. 125, 461–471.
Musson, F.M., Clarke, M.L., Wintle, A.G., 1994. Luminescence dating of loess from the Liujiapo section central China. Quat. Geochronol. 13, 407–410.
O'Neil, J.R., Clayton, R.N., Mayeda, T.K., 1969. Oxygen isotope fractionation in divalent metal carbonates. J. Chem. Phys. 51, 5547–5558.
Pye, K., Zhou, L.P., 1989. Late Pleistocene and Holocene aeolian dust deposition in North China and the northwest Pacific Ocean. Palaeogeogr., Palaeoclimatol., Palaeoecol. 73, 11–23.
Rossinsky Jr, V., Swart, P.K., 1993. Influence of climate on the formation and isotopic composition of calcretes. In: Swart, P.K., Lohmann, K.C., McKenzie, J., Savin, S. (Eds.), Climate Change in Continental Isotopic Records, Am. Geophys. Union Geophys. Monogr. 78, 67–75.
Rozanski, K., Araguás-Araguás, L., Gonfiantini, R., 1993. Isotopic patterns in modern global precipitation. In: Swart, P.K., Lohmann, K.C., McKenzie, J., Savin, S. (Eds.), Climate Change in Continental Isotopic Records, Am. Geophys. Union Geophys. Monogr. 78, 1–36.
Schwarcz, H.P., Latham, A.G., 1989. Dirty calcites 1: uranium series dating of contaminated calcite using leachates alone. Isotope Geosci. 80, 35–43.

Sun, J., Li, X., 1986. Palaeoenvironment of the last glacial (Dali) stage in North China. In: Gardiner, V., (Ed.), Int. Geomorp. 2, 763–773.

Sun, X.J., Song, C.Q., Wang, F.Y., Sun, M.R., 1997. Vegetation history of the Loess Plateau of China during the last 100,000 years based on pollen data. Quat. Int. 37, 25–36.

Szabo, B.J., McHugh, W.P., Schaber, G.G., Haynes, C.V., Breed, C.S., 1989. Uranium-series dated authigenic carbonates and Acheulian sites in Southern Egypt. Science 243, 1053–1056.

Teeri, J.A., Stowe, L.G., 1976. Climate patterns and the distribution of C4 grasses in North America. Oecologia 23, 1–12.

Thompson, R., Maher, B.A., 1995. Age models, sediment fluxes and palaeoclimatic reconstructions for the Chinese loess and palaeosol sequences. Geophys. J. Int. 123, 611–622.

Wang, Y., Zheng, S.H., 1989. Paleosol nodules as Pleistocene paleoclimatic indicators Luochuan P.R. China. Palaeogeogr., Palaeoclimatol., Palaeoecol. 76, 39–44.

Wang, H., Ambrose, S.H., Liu, C-L.J., Follmer, L.R., 1997. Paleosol stable isotope evidence for Early Hominid occupation of East Asian temperate environments. Quat. Res. 48, 228–238.

Wendt, I., Carl, C., 1991. The statistical distribution of the mean square weighted deviation. Chem. Geol. (Isotope Geosci.) 86, 275–285.

Wright, V.P., Tucker, M.E., 1991. In: Wright, V.P., Tucker, M.E. (Eds.), Calcretes vol. 2. International Association of Sedimentologists, pp. 1–22. reprint.

York, D., 1969. Least-squares fitting of a straight line with correlated errors. Earth Planet. Sci. Lett. 5, 320–324.

Zheng, S., Wang, Y., Chen, C., 1987. Studies on the stable isotopes in carbonates in Luochuan loess section: applicability of the Ca daduies as palaeoclimatic indicators. In: Tungsheng, L. (Ed.), Aspects of Loess Research. China Ocean Press, Beijing, pp. 283–290.